

# Circular RNA hsa\_circ\_0006168: A potential biomarker for the diagnosis and prognosis of prostate cancer

YE DING<sup>1\*</sup>, MAO-TONG LIU<sup>2\*</sup>, NA YU<sup>1</sup>, LIUSIJIE GAO<sup>3</sup> and LI-PING CHEN<sup>3</sup>

<sup>1</sup>Department of Medical Laboratory, Affiliated Hospital 2 of Nantong University, Nantong First People's Hospital, Nantong, Jiangsu 226000, P.R. China; <sup>2</sup>Department of Radiology, Affiliated Nantong Hospital 3 of Nantong University, Nantong Third People's Hospital, Nantong, Jiangsu 226000, P.R. China; <sup>3</sup>Center for Reproductive Medicine, Affiliated Hospital 2 of Nantong University, Nantong First People's Hospital, Nantong, Jiangsu 226000, P.R. China

Received May 20, 2025; Accepted December 9, 2025

DOI: 10.3892/ol.2026.15455

**Abstract.** The limited specificity of prostate-specific antigen for prostate cancer (PCa) necessitates novel, non-invasive biomarkers. The present study aimed to investigate the expression of the circular (circ)RNA hsa\_circ\_0006168 in PCa and its association with clinical parameters, and to evaluate its potential as a diagnostic and prognostic biomarker for PCa. Serum samples were collected from patients with PCa, benign prostatic hyperplasia (BPH) and healthy controls. Reverse transcription-quantitative PCR was used to measure the expression level of hsa\_circ\_0006168 in the sera. The association between the expression of hsa\_circ\_0006168 and several clinicopathological parameters was subsequently analyzed, and univariate and multivariate Cox regression analyses were performed to identify factors affecting prognosis. The expression level of hsa\_circ\_0006168 in the sera of patients with PCa was revealed to be significantly higher compared with that in the patients with BPH and the healthy controls. The area under the receiver operating characteristic curve was 0.773. The clinicopathological parameter analysis revealed that a high expression level of hsa\_circ\_0006168 was positively associated with the Gleason score, consistent with circRNA sequencing data. Cox regression analysis revealed that tumor-node-metastasis staging was an independent risk factor affecting prognosis. Furthermore, the expression level of hsa\_circ\_0006168, the Gleason score and bone metastasis were identified as significant risk factors according to the univariate Cox regression analysis; however, no significant factors were identified in the multivariate Cox regression analysis. In conclusion, serum hsa\_circ\_0006168

may be a promising biomarker for the early diagnosis and prognosis evaluation of PCa.

## Introduction

Prostate cancer (PCa) presents a major global health concern for men (1). The widely used biomarker, prostate-specific antigen (PSA), however, lacks the specificity to reliably distinguish cancer from benign conditions, such as benign prostatic hyperplasia and prostatitis. Consequently, elevated PSA levels frequently lead to unnecessary prostate biopsy, which are invasive procedures associated with potential complications including infection, bleeding, and significant patient anxiety (2). This difficulty highlights a pressing need for identifying biomarkers that better reflect the underlying tumor pathophysiology.

Circular (circ)RNAs, a class of non-coding RNAs that have been demonstrated to fulfil several key regulatory roles (3,4), are promising candidates as biomarkers due to their unique stability and presence in biological samples (5-7). Specifically, their covalently closed loop structure renders them resistant to exonuclease-mediated degradation, making them ideal candidates for liquid biopsy. Compared with traditional tissue biopsy, liquid biopsies based on stable circulating biomarkers offer a non-invasive, repeatable, and real-time method to monitor tumor dynamics, which is crucial for early detection and disease management.

Hsa\_circ\_0006168 has previously been reported as an oncogene in esophageal squamous cell carcinoma (ESCC) and glioblastoma (8,9). Therefore, it was hypothesized that it might also be dysregulated in PCa. The combination of data-driven evidence from PCa and functional reports in other cancers highlighted a critical research gap. Despite the growing interest in circRNAs (3-7), the specific expression profile and diagnostic potential of hsa\_circ\_0006168 in the context of prostatic malignancies remain largely unexplored. Therefore, the present study aimed to investigate the role and clinical significance of hsa\_circ\_0006168 in the pathophysiology of PCa. The present study is the first, to the best of our knowledge, to assess the expression level of hsa\_circ\_0006168 in serum samples from patients with PCa to explore its clinical significance as a biomarker for early diagnosis and prognosis evaluation.

---

*Correspondence to:* Professor Li-Ping Chen, Center for Reproductive Medicine, Affiliated Hospital 2 of Nantong University, Nantong First People's Hospital, 666 Shengli Road, Nantong, Jiangsu 226000, P.R. China  
E-mail: jichen0816@126.com

\*Contributed equally

*Key words:* prostate cancer, hsa\_circ\_0006168, biomarker

## Materials and methods

**Patients and serum samples.** The present study was approved by the Ethics Committee of Nantong First People's Hospital (Nantong, China; approval no. 2023-KY007-1). All patients provided written informed consent to participate specifically in the present research. A total of 90 patients with PCa from Nantong First People's Hospital, who were treated between October 2022 and May 2023, were recruited into the PCa group. The inclusion criteria were as follows: i) Confirmed diagnosis of PCa via biopsy; ii) first-time treatment of the patient, undergoing radical prostatectomy or other treatments, such as radiotherapy or chemotherapy; and iii) complete clinical data available. The exclusion criteria included the following: i) Diagnosis of other concurrent malignancies; ii) diagnosis of immune, infectious or acute diseases; iii) inadequate organ function; and iv) incomplete clinical data available. Additionally, 30 patients with benign prostatic hyperplasia (BPH) and 60 age-matched healthy individuals undergoing routine physical examination were enrolled as the BPH group and control group, respectively, during the same period. For the BPH group, inclusion criteria were: i) Clinically confirmed diagnosis of BPH. Exclusion criteria were: i) Evidence or suspicion of PCa (confirmed via histopathology or clinical assessment); ii) History of any malignancy; and iii) incomplete clinical data. For the control group, Inclusion criteria were: i) Age-matched individuals undergoing routine physical examination. Exclusion criteria were: i) History of malignancy; ii) known urological diseases; and iii) abnormal PSA levels or Digital Rectal Exam (DRE) results.

**RNA extraction and reverse transcription-quantitative PCR (RT-qPCR) assay.** Patient blood samples were collected in the morning after fasting, and 4 ml venous blood was drawn. The samples were subsequently centrifuged at 2,000 x g at 4°C for 10 min, and the supernatant was collected and placed in RNase-free microcentrifuge tubes. These tubes were stored at -80°C for later use. Total RNA was extracted using a plasma RNA extraction kit (BioTeke Corporation) and diluted with 30  $\mu$ l nuclease-free water per sample. Total RNA from the RWPE-1, LNCaP, DU145 and PC-3 cell lines was extracted using TRIzol (Invitrogen; Thermo Fisher Scientific, Inc.) according to the manufacturer's protocol. cDNA was synthesized from the total RNA using a BL699A Reverse Transcription kit (with DNase; cat. no. BL699A; Biosharp Life Sciences) with random hexamer primers under the following conditions: 25°C for 10 min, 42°C for 15 min and 85°C for 5 sec. All RNA and cDNA samples were stored at -80°C prior to subsequent analysis.

The relative expression of hsa\_circ\_0006168 was determined using a LightCycler® 480 Instrument II (Roche Diagnostics) with 2X Universal SYBR Green Fast qPCR Mix (cat. no. RK21203; Abclonal Biotech Co., Ltd.). The following thermocycling conditions were used: Initial denaturation at 95°C for 30 sec, followed by 45 cycles of denaturation at 95°C for 5 sec and annealing/extension at 60°C for 30 sec. The RT-qPCR primer sequences for hsa\_circ\_0006168 were specifically designed to span the back-splice junction to ensure amplification of the circular transcript. The sequences were as follows: Forward, 5'-TGCCAAGCTTCATAATCTGGT-3'

Table I. Intra- and inter assay coefficients of variation of hsa\_circ\_0006168 and GAPDH.

Parameter	hsa_circ_0006168	GAPDH
Intra-assay		
Mean $\pm$ SD	28.62 $\pm$ 0.37	18.35 $\pm$ 0.32
CV, %	1.46	1.85
Inter-assay		
Mean $\pm$ SD	28.90 $\pm$ 0.75	18.81 $\pm$ 0.53
CV, %	2.37	2.24

SD, standard deviation; CV, coefficient of variation.

and reverse, 5'-CCTTTGGCATCCCTATTAGTCTT-3', with an expected amplified product length of 60 bp. The identity of the amplicon spanning the back-splice junction was confirmed using Sanger sequencing (Fig. S1). For GAPDH, the RT-qPCR primers were as follows: Forward, 5'-CCTTCATTGACCTCAACTA-3' and reverse, 5'-TGGGAAGATGGTGATGGGATT-3'. The relative expression levels were calculated using the  $2^{-\Delta\Delta C_q}$  method (10), with GAPDH as the internal control.

**Cell culture.** The human normal prostatic epithelial cell line RWPE-1, and the PCa cell lines PC-3, DU-145 and LNCaP, were cultured in RPMI-1640 medium (Invitrogen™; Thermo Fisher Scientific, Inc.) supplemented with 10% fetal bovine serum (Gibco; Thermo Fisher Scientific, Inc.) at 37°C in a humidified atmosphere containing 5% CO<sub>2</sub>. To validate hsa\_circ\_0006168 expression *in vitro*, total RNA was extracted from these cells and analyzed via the RT-qPCR method described above.

**Bioinformatics analysis.** CircRNA expression data and the clinical information of PCa tissue samples were retrieved from the Gene Expression Omnibus (GEO) database (ncbi.nlm.nih.gov/geo/) datasets GSE113153 (11) and GSE155792. The GSE113153 dataset comprised data from five pairs of PCa tissues, with samples categorized based on the Gleason score (12): >8, poorly differentiated cancer; and <6, well-differentiated cancer. The GSE155792 dataset included the data from one PCa tissue and its adjacent normal tissue. Differential expression analysis was performed using R software (version 4.3.2; The R Foundation), with the criteria set as log<sub>2</sub> fold change  $\geq$ 1 and P $\leq$ 0.05 for identifying differentially expressed circRNAs.

**Database analysis.** The target genes of hsa\_circ\_0006168 were predicted using the Cancer-Specific CircRNA Database (<http://gb.whu.edu.cn/CSCD/>). To determine the potential biological functions of differentially expressed mRNAs in the competing endogenous (ce)RNA network in PCa, Gene Ontology (GO) and Kyoto Encyclopedia of Genes and Genomes (KEGG) functional enrichment analyses were performed using the ClusterProfiler package in R software (version 4.3.2; R Foundation for Statistical Computing). To identify differentially expressed microRNAs (miRNAs/miRs), miRNA expression data from two public GEO datasets were also analyzed: GSE119338 (13) and GSE14857 (14).

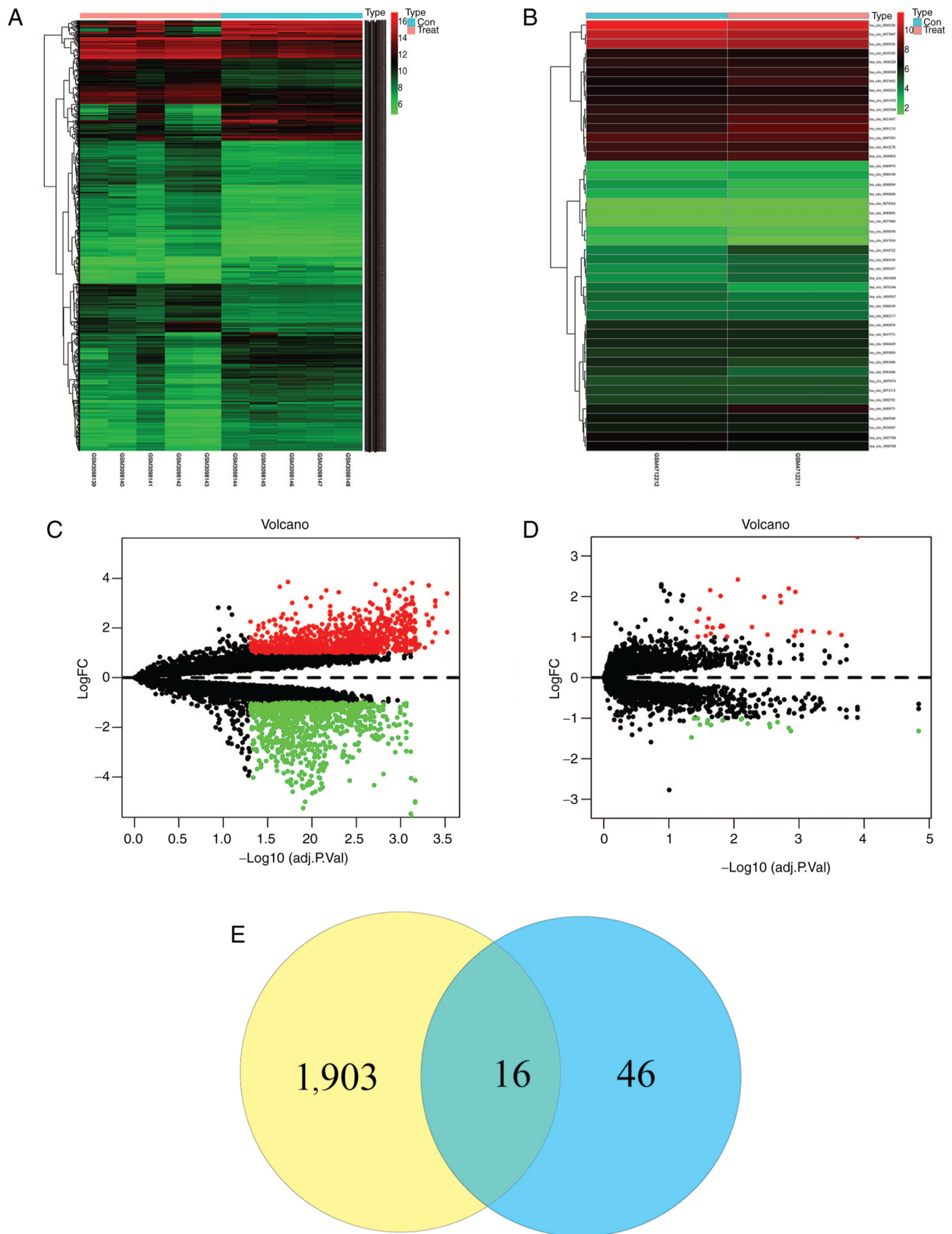


Figure 1. Identification of differentially expressed circRNAs in prostate cancer. Heatmaps of (A) GSE15792 and (B) GSE113153 datasets. Volcano plots of the (C) GSE15792 and (D) GSE113153 datasets. (E) Venn diagram based on the intersection of the differentially expressed genes. FC, fold change.

**Statistical analysis.** Statistical analysis was performed using SPSS 20.0 (IBM Corp.) and R software (version 4.3.2; The R Foundation). Measurement data with a normal distribution are expressed as the mean  $\pm$  SD. Unpaired t-test was utilized

to compare differences between two groups. For comparisons among three or more groups, one-way analysis of variance was performed, followed by Tukey's post hoc test. Correlation analysis was performed using Pearson's correlation test. The  $\chi^2$  test

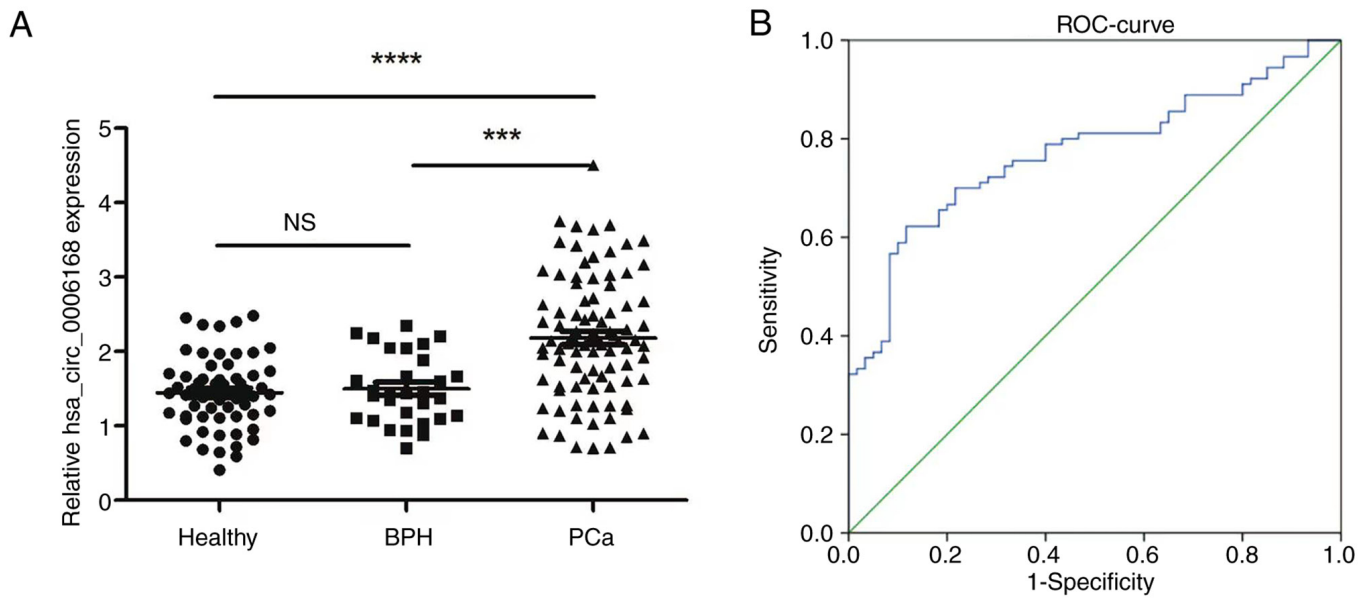


Figure 2. Expression levels and diagnostic value of serum hsa\_circ\_0006168 in patients with PCa. (A) Expression levels of hsa\_circ\_0006168 in the sera of patients with PCa or BPH, and healthy controls. (B) hsa\_circ\_0006168 was shown to have good diagnostic value as a PCa biomarker. \*\*\* $P < 0.001$ ; \*\*\*\* $P < 0.0001$ . PCa, prostate cancer; BPH, benign prostatic hyperplasia; NS, not significant; ROC, Receiver Operating Characteristic.

was used to analyze the association between hsa\_circ\_0006168 levels and the clinicopathological features of patients with PCa. The survival package in R software (version 4.3.2) was used to perform univariate and multivariate Cox regression analysis of clinicopathological factors and hsa\_circ\_0006168 expression levels. Additionally, nomograms and survival curves were plotted to determine whether clinicopathological factors and hsa\_circ\_0006168 expression levels could serve as independent prognostic indicators.  $P < 0.05$  was considered to indicate a statistically significant difference.

## Results

*Upregulation of hsa\_circ\_0006168 in the serum of patients with PCa.* Bioinformatics analysis of the public GEO datasets GSE155792 and GSE113153 identified hsa\_circ\_0006168 as a significantly upregulated circRNA in PCa tissues (Fig. 1). To validate this finding, the expression level of serum hsa\_circ\_0006168 was assessed in patients with PCa, which demonstrated that the serum levels of hsa\_circ\_0006168 was significantly elevated compared with in patients with BPH and healthy controls (Fig. 2A). Furthermore, hsa\_circ\_0006168 expression levels were evaluated in the normal prostatic epithelial cell line RWPE-1, and the PCa cell lines LNCaP, DU145 and PC-3. The results demonstrated that the expression of hsa\_circ\_0006168 was significantly elevated in the DU145 and PC-3 cell lines compared with the normal RWPE-1 cell line (Fig. 3).

*Diagnostic value of serum hsa\_circ\_0006168.* To evaluate the diagnostic potential of serum hsa\_circ\_0006168, receiver operating characteristic curve analysis was performed. Serum hsa\_circ\_0006168 was revealed to demonstrate good diagnostic performance in distinguishing patients with PCa from controls, with an area under the curve of 0.773 (95% confidence

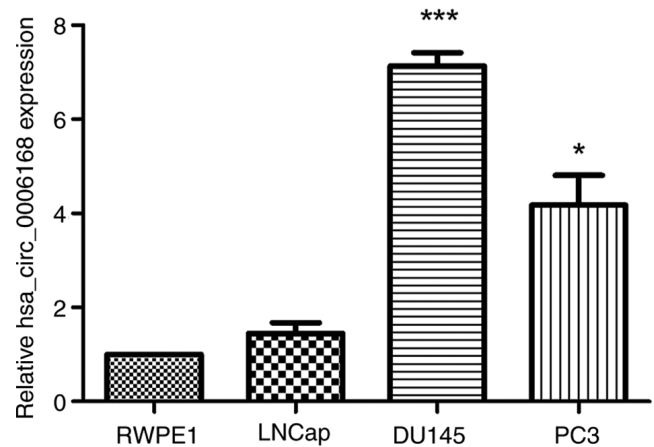


Figure 3. Expression of hsa\_circ\_0006168 in the cell lines utilized in the present study. \* $P < 0.05$ ; \*\*\* $P < 0.001$  vs. RWPE-1.

interval, 0.698-0.847), a sensitivity of 74.4% and a specificity of 88.3% at the optimal cut-off value (Fig. 2B).

*Evaluation of hsa\_circ\_0006168 detection in the serum.* RT-qPCR for detecting serum hsa\_circ\_0006168 was performed, and the analysis was demonstrated to be highly reliable: The assay demonstrated marked linearity ( $R^2 = 0.9943$ ) and high reproducibility (Fig. 4A and B; Table I). Notably, in terms of clinical application, hsa\_circ\_0006168 levels were revealed to remain stable in serum samples exposed to prolonged ambient temperatures and multiple freeze-thaw cycles (Fig. 4C and D), confirming its suitability as a liquid biopsy biomarker.

*Association with clinicopathological factors.* Analysis of clinicopathological parameters revealed that a high expression

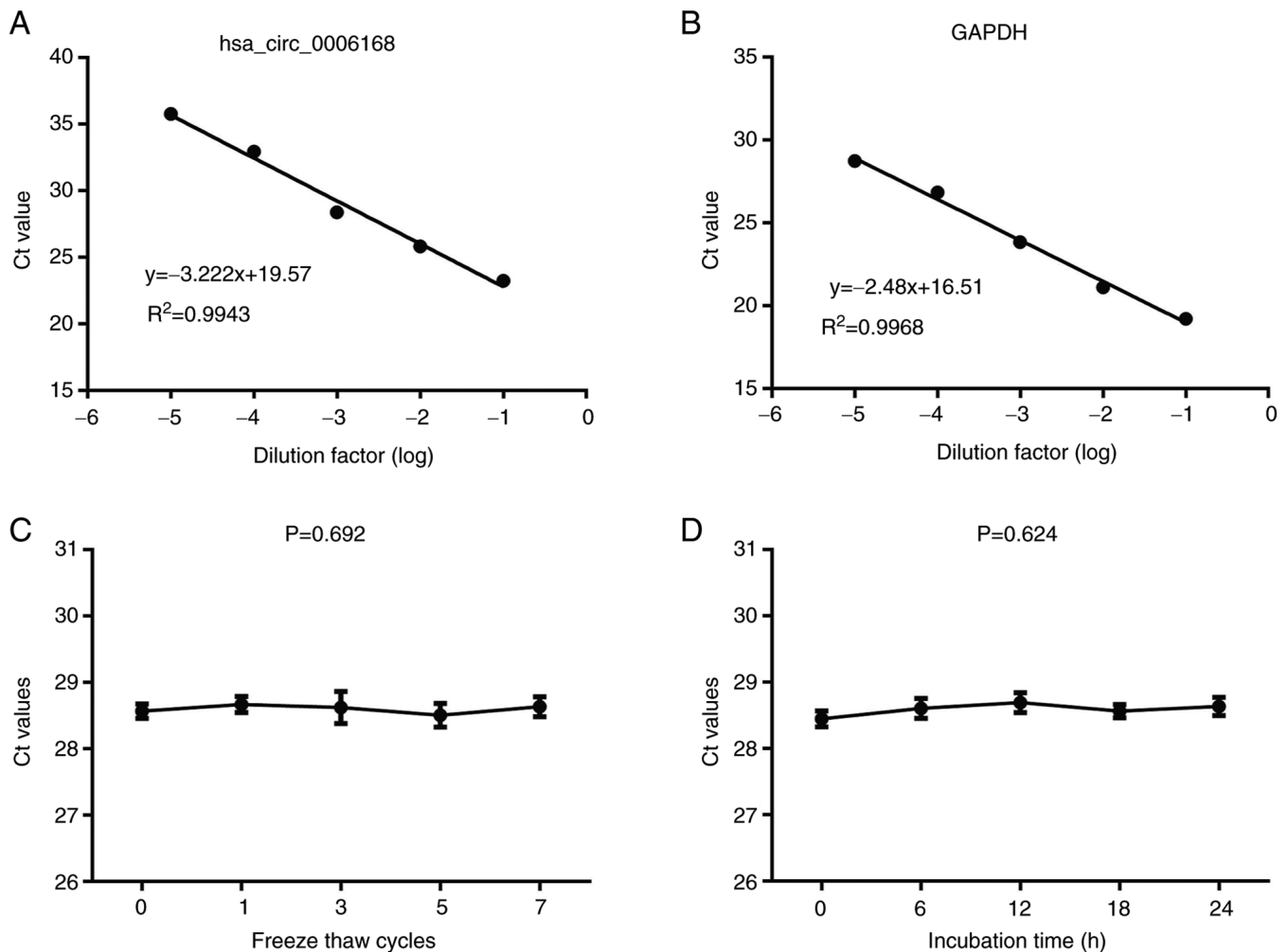


Figure 4. Methodological evaluation of hsa\_circ\_0006168. The linearity of (A) hsa\_circ\_0006168 and (B) GAPDH were found to be acceptable. The stability of hsa\_circ\_0006168 (C) after repeated freezing and thawing, and (D) at room temperature.

of hsa\_circ\_0006168 was significantly associated with higher Gleason scores, suggesting an association with worse tumor differentiation, and therefore, indicating its potential role in PCa progression. However, no significant associations were demonstrated between a high expression of the circRNA and age, tumor-node-metastasis (TNM) stage (15), bone metastasis or PSA level (Table II).

**Cox regression analysis of prognostic factors.** In the univariate Cox regression analysis, the TNM stage, Gleason score, presence of bone metastasis and high expression of hsa\_circ\_0006168 were all revealed to be significant predictors of poor prognosis. However, in the multivariate analysis, only the TNM stage remained as an independent prognostic factor (Table III). A nomogram was then constructed based on these factors, which demonstrated a strong discriminative ability for predicting patient survival (C-index, 0.7886), with good calibration and clinical utility (Fig. 5A-C). Kaplan-Meier survival analysis demonstrated that patients with high hsa\_circ\_0006168 expression had significantly poorer overall survival compared with the low expression group (Fig. 5D).

**Exploration of the potential underlying regulatory mechanism.** To explore potential mechanisms, a preliminary bioinformatics

analysis was performed. GO and KEGG enrichment analyses of predicted target genes for hsa\_circ\_0006168 indicated a primary association with the p53 signaling pathway (Fig. 6A and B; Table IV). Moreover, the sequence and predicted structure of hsa\_circ\_0006168 were identified (Fig. 6C). The analysis of two public miRNA datasets then identified several differentially expressed miRNAs (Tables V and VI), with miR-205 noted in both (Fig. 6D), suggesting it as a potential interaction partner. Collectively, these exploratory *in silico* findings form a working hypothesis that hsa\_circ\_0006168 may function via the p53 pathway and/or by sponging miR-205, a hypothesis that requires future experimental validation.

**Discussion**

PCa is a leading cause of morbidity and mortality among men worldwide, with an estimated 1.5 million new cases and 397,000 deaths reported in 2022 (1). Although several treatment options have been reported to notably improve outcomes in early-stage disease, advanced PCa with distant metastasis remains challenging to manage (2). Therefore, there is a pressing need to explore novel diagnostic and therapeutic approaches to enable both early detection of the disease and the design of personalized treatment strategies.

Table II. Association between hsa\_circ\_0006168 expression and clinicopathological features of patients with prostate cancer.

Characteristic	Total (n=90) (%)	hsa_circ_0006168 expression		$\chi^2$ value	P-value
		Low (n=32) (%)	High (n=58) (%)		
Age				0.148	0.700
>60 years	51 (56.7)	19 (59.4)	32 (55.2)		
≤60 years	39 (43.3)	13 (40.6)	26 (44.8)		
PSA, ng/ml				0.170	0.680
>4	48 (53.3)	18 (56.2)	30 (51.7)		
<4	42 (46.7)	14 (43.8)	28 (48.3)		
Gleason score				4.098	0.043 <sup>a</sup>
≥7	60 (66.7)	17 (53.1)	43 (74.1)		
<7	30 (33.7)	15 (46.9)	15 (25.9)		
Bone metastasis				0.030	0.862
Yes	32 (35.6)	11 (34.4)	21 (36.2)		
No	58 (64.4)	21 (65.6)	37 (63.8)		
TNM stage				0.357	0.550
I and II	46 (51.1)	15 (46.9)	31 (53.4)		
III and IV	44 (48.9)	17 (53.1)	27 (46.6)		

<sup>a</sup>P<0.05. PSA, prostate-specific antigen; TNM, tumor-node-metastasis.

Hsa\_circ\_0006168 (alternatively known as circCNOT6L) is located at chr4:78694234-78697546 and has a length of 3,312 nucleotides. It was first identified by Shi *et al* (8), who revealed that hsa\_circ\_0006168 expression is markedly elevated in ESCC tissues and cell lines compared with that in normal controls, and its high expression was associated with lymph node metastasis and advanced TNM staging in patients with ESCC. The present study screened for differentially expressed circRNAs using publicly available circRNA expression data, and the findings were validated in serum samples. The results obtained demonstrated that the expression level of hsa\_circ\_0006168 was significantly higher in the serum of patients with PCa compared with that in BPH and healthy controls, suggesting the potential of hsa\_circ\_0006168 as a non-invasive diagnostic biomarker for PCa.

Moreover, a positive association was observed between high hsa\_circ\_0006168 expression and the Gleason score, demonstrating that elevated hsa\_circ\_0006168 levels are associated with lower PCa differentiation and a worse prognosis. Furthermore, hsa\_circ\_0006168 expression levels were evaluated in the normal prostatic epithelial cell line RWPE-1, and the PCa cell lines LNCaP, DU145 and PC-3. Notably, the expression of hsa\_circ\_0006168 was demonstrated to be significantly elevated in the DU145 and PC-3 cell lines, which are androgen-independent, poorly differentiated and exhibit high metastatic potential (16). This increased expression may be associated with androgen receptor (AR) activity as AR positivity is strongly associated with castration-resistant prostate cancer (CRPC). In this cancer type, traditional endocrine therapy remains effective for 18-24 months (17); however, disease progression, driven by AR mutations and even low androgen levels, can promote PCa malignancy (18). The bioinformatics analysis performed in the present study predicted

that the target genes of hsa\_circ\_0006168 are enriched in the p53 signaling pathway. In PCa, inactivation of p53 is a key event that drives tumor progression, metastasis and therapeutic resistance, making it a critical biomarker throughout the natural history of the disease (19-21). Future studies should use larger sample sizes and diverse ethnic and geographical representation, and employ knockdown or overexpression of hsa\_circ\_0006168 experiments. Moreover, its interaction with ARs should be investigated both *in vitro* and *in vivo* to elucidate its regulatory role in PCa progression.

CircRNAs are widely distributed in eukaryotic cells and contain multiple miRNA response elements, enabling them to act as ceRNAs through competitively binding to miRNAs (22). Following processing by nucleases, mature miRNAs are assembled into RNA-induced silencing complexes, where they target mRNAs via base-pairing complementarity, leading to mRNA degradation or translational repression (23-25). As ceRNAs, circRNAs can mitigate the inhibitory effects of miRNAs on target mRNAs, thereby regulating the expression and function of associated genes. For example, a bioinformatics analysis performed previously predicted that circGNG4 can enhance EYA transcriptional coactivator and phosphatase 3/c-Myc expression through sponging miR-223, thereby promoting the malignant progression of PCa (26). Similarly, Chao *et al* (27) performed a fluorescence *in situ* hybridization analysis to localize a novel circRNA, circSOBP, primarily in the cytoplasm of PCa cells, where its overexpression was reported to inhibit cell invasion and migration. Dual-luciferase assays reported that circSOBP could also bind to miR-141-3p, thereby modulating the myosin phosphatase target subunit 1/phosphorylated myosin regulatory light chain 2 axis to suppress PCa progression. The finding in the present study that hsa\_circ\_0006168 is upregulated and associated with

Table III. Univariate and multivariate Cox regression analysis of hsa\_circ\_0006168 expression levels and clinicopathological factors.

Variable	Univariate analysis		Multivariate analysis	
	HR (95% CI)	P-value	HR (95% CI)	P-value
hsa_circ_0006168 expression	2.989 (1.235-7.227)	0.015	2.114 (0.858-5.212)	0.104
Age	0.632 (0.332-1.203)	0.191	-	-
TNM stage	7.017 (3.028-16.233)	<0.001	4.958 (1.811-13.577)	0.002
Gleason score	2.697 (1.033-7.047)	0.041	2.404 (0.866-6.669)	0.092
Bone metastasis	2.687 (1.355-5.327)	0.005	1.311 (0.634-2.710)	0.465
PSA	0.918 (0.465-1.812)	0.805	-	-

HR, hazard ratio; CI, confidence interval; TNM, tumor-node-metastasis; PSA, prostate-specific antigen.

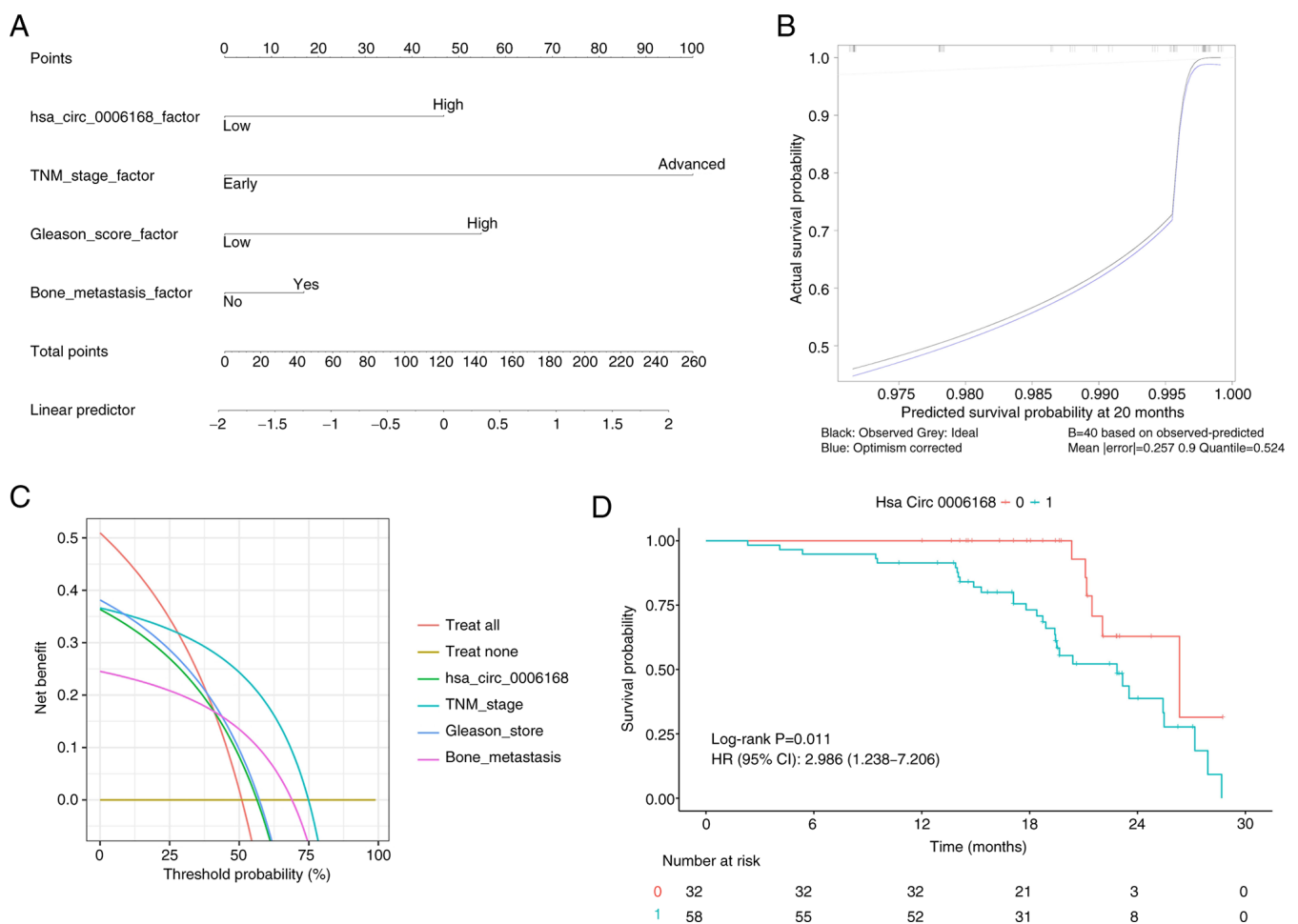


Figure 5. Construction and evaluation of a nomogram for predicting overall survival in patients with prostate cancer. (A) Nomogram for predicting survival probability. (B) Calibration curve for survival prediction at 20 months. (C) Decision curve analysis, highlighting clinical utility. (D) Kaplan-Meier survival curves for patients with prostate cancer, stratified according to the expression levels of hsa\_circ\_0006168. TNM, tumor-node-metastasis; HR, hazard ratio; CI, confidence interval.

more aggressive features of PCa is consistent with the oncogenic roles reported for other circRNAs within this specific cancer type. For example, circHIPK3 has been reported to be overexpressed in PCa, where it promotes cell proliferation and invasion by acting as a ceRNA to sponge miR-193a-3p (11). Similarly, circ0005276 has also been reported to be upregulated

in PCa tissues and facilitates cell proliferation and migration. However, it functions through a different mechanism by interacting with the Fused in Sarcoma protein to transcriptionally activate X-linked Inhibitor of Apoptosis (28). This suggests that a class of circRNAs may typically be involved in the malignant progression of PCa. However, in comparison

Table IV. Gene Ontology and Kyoto Encyclopedia of Genes and Genomes analysis of downstream target genes associated with hsa\_circ\_0006168.

ID	Description	Gene ID	P-value
GO:0003712	Transcription coregulator activity	HMGB2/ZBTB18/HCFC2/YAF2/MIER1/PHF12/HMGA1/HNRNPU/RYBP/ATXN7L3/LIMD1/KMT2D/SETD3/RCOR1/DDIT3/BTG1/SOX12/RBM14/TMF1/NPAT/TCERG1/BCL9L/CTNNB1	0.000264
GO:0017016	Ras GTPase binding	CDC42EP1/CDC42SE1/PREX2/RNF41/RCC2/TMEM127/PARD6B/FGD4/RASGRP1/ARHGEF28/TIAM1/TNPO1/APIG1/ABI2/PLEKHG5/BICD2/TBC1D16/HACE1/RAB11FIP4/KCTD10/NET1/EXOC2	5.01x10 <sup>-5</sup>
GO:0031267	Small GTPase binding	CDC42EP1/CDC42SE1/PREX2/RNF41/RCC2/TMEM127/PARD6B/FGD4/RASGRP1/ARHGEF28/TIAM1/TNPO1/APIG1/ABI2/PLEKHG5/BICD2/TBC1D16/HACE1/RAB11FIP4/KCTD10/NET1/EXOC2	7.89x10 <sup>-5</sup>
GO:0140297	DNA-binding transcription factor binding	HIF1A/RARB/ACTB/FOS/MIER1/SP1/HMGA1/GTF2I/DHX33/CRTC3/ETS2/RB1/SETD3/DDIT3/ESR1/TMF1/TCF12/TCERG1/FOXP1/CTNNB1	3.46x10 <sup>-5</sup>
GO:0003713	Transcription coactivator activity	HMGB2/ZBTB18/HCFC2/YAF2/HMGA1/ATXN7L3/KMT2D/SETD3/DDIT3/SOX12/RBM14/TMF1/NPAT/TCERG1/BCL9L/CTNNB1	0.000133
GO:0061629	RNA polymerase II-specific DNA-binding transcription factor binding	HIF1A/RARB/ACTB/FOS/MIER1/SP1/HMGA1/GTF2I/ETS2/RB1/SETD3/ESR1/TMF1/TCERG1/FOXP1/CTNNB1	0.000133
GO:0017048	Rho GTPase binding	CDC42EP1/CDC42SE1/PREX2/RCC2/PARD6B/FGD4/ARHGEF28/TIAM1/ABI2/PLEKHG5/HACE1/KCTD10/NET1	3.02x10 <sup>-5</sup>
GO:0008022	Protein C-terminus binding	PRKAA1/YWHAQ/CD2AP/PRRC2C/DAB2/FOXN3/SP1/DLG4/FIGN/RBFOX1/NPAT/CTNNB1	0.000542
GO:0003730	mRNA 3'-UTR binding	HNRNPR/ELAVL4/NOVA1/SERBP1/HNRNPU/ZFP36L2/CPEB2/RNPS1/ZFP36L1	0.000683
GO:0010485	H4 histone acetyltransferase activity	KANSL1L/NAA50/KANSL1/NAA40	0.000334
hsa04010	MAPK signaling pathway	HSPA1B/RPS6KA6/CSF1R/CRKL/ERBB3/MAX/FOS/EPHA2/TRADD/MKNK2/RAP1B/PPP3R1/RASGRP1/MAP3K4/DDIT3/MAPK1/GADD45A/RAC3/TAOK1/MAP3K7	1.22x10 <sup>-5</sup>
hsa04218	Cellular senescence	CDKN1A/E2F3/CALM2/PTEN/CCND2/CHEK1/CCNE1/PPP3R1/RB1/ZFP36L2/HIPK3/ZFP36L1/MAPK1/GADD45A/PPP1CB	2.59x10 <sup>-6</sup>
hsa05166	Human T cell leukemia virus 1 infection	CDKN1A/CREB5/E2F3/FOS/PTEN/CCND2/CHEK1/CCNE1/PPP3R1/CRTC3/ETS2/RB1/MAPK1/NRP1	0.000564
hsa05224	Breast cancer	FZD6/CDKN1A/E2F3/FOS/PTEN/SP1/RB1/ESR1/MAPK1/GADD45A/JAG1/FRAT2/CTNNB1	3.04x10 <sup>-5</sup>
hsa05203	Viral carcinogenesis	YWHAQ/YWHAZ/CDKN1A/CREB5/CCND2/TRADD/CHEK1/CCNE1/TRAF1/RB1/YWHAZ/EPHA2/SH2B3/SH2B1/SH2B2/SH2B3/SH2B4/SH2B5/SH2B6/SH2B7/SH2B8/SH2B9/SH2B10/SH2B11/SH2B12/SH2B13/SH2B14/SH2B15/SH2B16/SH2B17/SH2B18/SH2B19/SH2B20/SH2B21/SH2B22/SH2B23/SH2B24/SH2B25/SH2B26/SH2B27/SH2B28/SH2B29/SH2B30/SH2B31/SH2B32/SH2B33/SH2B34/SH2B35/SH2B36/SH2B37/SH2B38/SH2B39/SH2B40/SH2B41/SH2B42/SH2B43/SH2B44/SH2B45/SH2B46/SH2B47/SH2B48/SH2B49/SH2B50/SH2B51/SH2B52/SH2B53/SH2B54/SH2B55/SH2B56/SH2B57/SH2B58/SH2B59/SH2B60/SH2B61/SH2B62/SH2B63/SH2B64/SH2B65/SH2B66/SH2B67/SH2B68/SH2B69/SH2B70/SH2B71/SH2B72/SH2B73/SH2B74/SH2B75/SH2B76/SH2B77/SH2B78/SH2B79/SH2B80/SH2B81/SH2B82/SH2B83/SH2B84/SH2B85/SH2B86/SH2B87/SH2B88/SH2B89/SH2B90/SH2B91/SH2B92/SH2B93/SH2B94/SH2B95/SH2B96/SH2B97/SH2B98/SH2B99/SH2B100	0.000804
hsa04110	Cell cycle	ORC4/YWHAQ/YWHAZ/CDKN1A/E2F3/CCND2/CHEK1/CCNE1/RB1/YWHAZ/EPHA2/SH2B3/SH2B1/SH2B2/SH2B4/SH2B5/SH2B6/SH2B7/SH2B8/SH2B9/SH2B10/SH2B11/SH2B12/SH2B13/SH2B14/SH2B15/SH2B16/SH2B17/SH2B18/SH2B19/SH2B20/SH2B21/SH2B22/SH2B23/SH2B24/SH2B25/SH2B26/SH2B27/SH2B28/SH2B29/SH2B30/SH2B31/SH2B32/SH2B33/SH2B34/SH2B35/SH2B36/SH2B37/SH2B38/SH2B39/SH2B40/SH2B41/SH2B42/SH2B43/SH2B44/SH2B45/SH2B46/SH2B47/SH2B48/SH2B49/SH2B50/SH2B51/SH2B52/SH2B53/SH2B54/SH2B55/SH2B56/SH2B57/SH2B58/SH2B59/SH2B60/SH2B61/SH2B62/SH2B63/SH2B64/SH2B65/SH2B66/SH2B67/SH2B68/SH2B69/SH2B70/SH2B71/SH2B72/SH2B73/SH2B74/SH2B75/SH2B76/SH2B77/SH2B78/SH2B79/SH2B80/SH2B81/SH2B82/SH2B83/SH2B84/SH2B85/SH2B86/SH2B87/SH2B88/SH2B89/SH2B90/SH2B91/SH2B92/SH2B93/SH2B94/SH2B95/SH2B96/SH2B97/SH2B98/SH2B99/SH2B100	0.000141
hsa04934	Cushing syndrome	FZD6/CDKN1A/CREB5/E2F3/RAP1B/CCNE1/SP1/KMT2D/RB1/MAPK1/CTNNB1	0.000844
hsa04390	Hippo signaling pathway	FZD6/YWHAQ/YWHAZ/ACTB/CCND2/PARD6B/DLG4/LIMD1/YWHAZ/EPHA2/SH2B3/SH2B1/SH2B2/SH2B4/SH2B5/SH2B6/SH2B7/SH2B8/SH2B9/SH2B10/SH2B11/SH2B12/SH2B13/SH2B14/SH2B15/SH2B16/SH2B17/SH2B18/SH2B19/SH2B20/SH2B21/SH2B22/SH2B23/SH2B24/SH2B25/SH2B26/SH2B27/SH2B28/SH2B29/SH2B30/SH2B31/SH2B32/SH2B33/SH2B34/SH2B35/SH2B36/SH2B37/SH2B38/SH2B39/SH2B40/SH2B41/SH2B42/SH2B43/SH2B44/SH2B45/SH2B46/SH2B47/SH2B48/SH2B49/SH2B50/SH2B51/SH2B52/SH2B53/SH2B54/SH2B55/SH2B56/SH2B57/SH2B58/SH2B59/SH2B60/SH2B61/SH2B62/SH2B63/SH2B64/SH2B65/SH2B66/SH2B67/SH2B68/SH2B69/SH2B70/SH2B71/SH2B72/SH2B73/SH2B74/SH2B75/SH2B76/SH2B77/SH2B78/SH2B79/SH2B80/SH2B81/SH2B82/SH2B83/SH2B84/SH2B85/SH2B86/SH2B87/SH2B88/SH2B89/SH2B90/SH2B91/SH2B92/SH2B93/SH2B94/SH2B95/SH2B96/SH2B97/SH2B98/SH2B99/SH2B100	0.000938
hsa05160	Hepatitis C	YWHAQ/YWHAZ/CDKN1A/E2F3/TRADD/OCLN/RB1/YWHAZ/EPHA2/SH2B3/SH2B1/SH2B2/SH2B4/SH2B5/SH2B6/SH2B7/SH2B8/SH2B9/SH2B10/SH2B11/SH2B12/SH2B13/SH2B14/SH2B15/SH2B16/SH2B17/SH2B18/SH2B19/SH2B20/SH2B21/SH2B22/SH2B23/SH2B24/SH2B25/SH2B26/SH2B27/SH2B28/SH2B29/SH2B30/SH2B31/SH2B32/SH2B33/SH2B34/SH2B35/SH2B36/SH2B37/SH2B38/SH2B39/SH2B40/SH2B41/SH2B42/SH2B43/SH2B44/SH2B45/SH2B46/SH2B47/SH2B48/SH2B49/SH2B50/SH2B51/SH2B52/SH2B53/SH2B54/SH2B55/SH2B56/SH2B57/SH2B58/SH2B59/SH2B60/SH2B61/SH2B62/SH2B63/SH2B64/SH2B65/SH2B66/SH2B67/SH2B68/SH2B69/SH2B70/SH2B71/SH2B72/SH2B73/SH2B74/SH2B75/SH2B76/SH2B77/SH2B78/SH2B79/SH2B80/SH2B81/SH2B82/SH2B83/SH2B84/SH2B85/SH2B86/SH2B87/SH2B88/SH2B89/SH2B90/SH2B91/SH2B92/SH2B93/SH2B94/SH2B95/SH2B96/SH2B97/SH2B98/SH2B99/SH2B100	0.000938

Table IV. Continued.

ID	Description	Gene ID	P-value
hsa04114	Oocyte meiosis	YWHAQ/YWHAZ/RPS6KA6/CALM2/CCNE1/PPP3R1/CPEB2/YWHAE/MAPK1/PPP1CB	0.000827
hsa05222	Small cell lung cancer	CDKN1A/RARB/E2F3/MAX/PTEN/CCNE1/TRAF1/RB1/GADD45A	0.000244
hsa04115	p53 signaling pathway	CDKN1A/RRM2/PTEN/CCND2/SESN3/CHEK1/CCNE1/GADD45A	0.000248

GO, Gene Ontology; UTR, untranslated region.

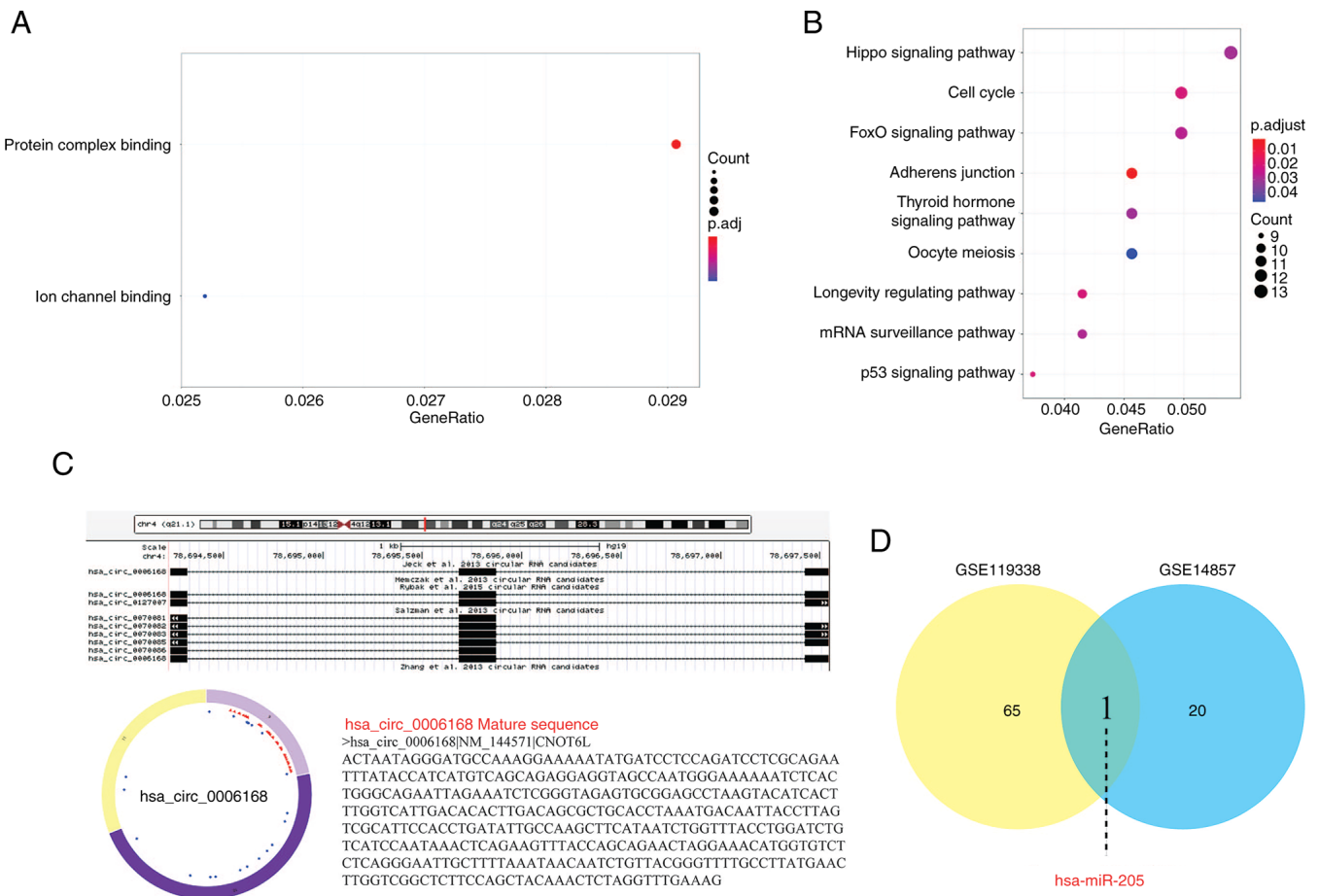


Figure 6. Bioinformatics analysis of the function, structure and targets of hsa\_circ\_0006168. (A) Gene Ontology and (B) Kyoto Encyclopedia of Genes and Genomes pathway analysis of hsa\_circ\_0006168. (C) Sequence and structural analysis of hsa\_circ\_0006168. (D) Differential microRNA analysis in prostate cancer tissue and cells.

with the aforementioned studies, the present study is the first to have characterized hsa\_circ\_0006168 as a non-invasive, serum-detectable marker, and also to have associated it with the AR/miR-205 axis, to the best of our knowledge, thereby providing a unique perspective on its role in PCa.

In the present study, differentially expressed miRNAs in PCa tissues and cells were analyzed using miRNA expression data from the datasets GSE119338 and GSE14857, identifying a downregulation in miR-205 expression. This finding aligns with an previous study by Gandellini *et al* (29), who reported

a decreased expression of miR-205 in PCa cells and tissues, demonstrating its tumor-suppressive role through inhibiting epithelial-mesenchymal transition. Hagman *et al* (30) further reported that miR-205 binds to the 3'-untranslated region of the AR, reducing both the transcription and protein levels of the AR, suggesting the therapeutic potential of miR-205 in CRPC. Additionally, Kalogirou *et al* (31) reported that squalene epoxidase (SQLE) and several cholesterol biosynthesis enzymes are overexpressed in advanced PCa, which was associated with poor survival. They also reported that miR-205

Table V. Differentially expressed miRs in the GSE119338 dataset.

Gene	logFC	P-value	Gene regulation
hsa-miR-034c	1.88339	0.002460	Down
hsa-miR-376b	1.81105	0.003005	Down
hsa-miR-376a	1.77345	0.003255	Down
hsa-miR-368	1.71005	0.003275	Down
hsa-miR-030a 3p	1.67436	0.003350	Down
hsa-miR-137	1.63115	0.003378	Down
hsa-miR-133a	1.72425	0.003670	Down
hsa-miR-210	1.83033	0.003706	Down
hsa-miR-034b	1.65755	0.003752	Down
hsa-miR-193b	1.61622	0.003861	Down
hsa-miR-133b	1.63867	0.004235	Down
hsa-miR-022	1.91686	0.004770	Down
hsa-miR-205	2.08786	0.004826	Down
hsa-miR-203	1.99239	0.004882	Down
hsa-miR-031	1.98816	0.005144	Down
hsa-miR-030e 3p	1.49580	0.005833	Down
hsa-miR-010b	1.53879	0.005835	Down
hsa-miR-030d	1.53824	0.006043	Down
hsa-miR-030e 5p	1.83719	0.006113	Down
hsa-miR-030c	1.59348	0.006288	Down
hsa-miR-024	1.74432	0.006604	Down
hsa-miR-001	1.50516	0.006745	Down
hsa-miR-152	1.70493	0.006880	Down
hsa-miR-030a 5p	1.49181	0.007102	Down
hsa-miR-224	1.92611	0.007991	Down
hsa-miR-423	1.64733	0.009312	Down
hsa-miR-365-1	1.58153	0.009464	Down
hsa-miR-030b	1.34008	0.010272	Down
hsa-miR-424	1.45159	0.010713	Down
hsa-miR-029c	1.56767	0.010900	Down
hsa-miR-449	1.27469	0.013276	Down
hsa-miR-221	1.38374	0.013456	Down
hsa-miR-503	1.33977	0.013816	Down
hsa-miR-027b	1.53227	0.014072	Down
hsa-miR-023a	1.47580	0.014885	Down
hsa-miR-135b	1.72096	0.015631	Down
hsa-miR-452	1.41561	0.019488	Down
hsa-miR-021	1.57238	0.019811	Down
hsa-miR-023b	1.40925	0.020878	Down
hsa-miR-027a	1.34136	0.022885	Down
hsa-miR-029a	1.27442	0.026287	Down
hsa-miR-095	1.16648	0.028329	Down
hsa-miR-149	1.19165	0.028613	Down
hsa-miR-034a	1.08216	0.029093	Down
hsa-miR-193	1.43661	0.030047	Down
hsa-miR-222	1.15869	0.033629	Down
hsa-miR-029b	1.40342	0.034209	Down
hsa-miR-107	1.02251	0.037370	Down
hsa-miR-009	1.21235	0.040226	Down
hsa-miR-130a	1.39363	0.041765	Down
hsa-miR-189	1.20643	0.045449	Down

Table V. Continued.

Gene	logFC	P-value	Gene regulation
hsa-miR-130b	1.25535	0.049841	Down
hsa-miR-103-1-pre	1.65357	0.022734	Up
hsa-miR-452-pre	1.65577	0.023460	Up
hsa-miR-491-pre	1.49639	0.030418	Up
hsa-miR-485-pre	1.58863	0.036311	Up
hsa-miR-492-pre	1.24900	0.037825	Up
hsa-miR-512-1-pre	1.33137	0.037889	Up
hsa-miR-506-pre	1.54105	0.043464	Up
hsa-miR-495-pre	1.33179	0.043764	Up
hsa-miR-485-3p	1.11936	0.044769	Up
hsa-miR-512-5p	1.07008	0.045630	Up
hsa-miR-513-2-pre	1.10115	0.047218	Up
hsa-miR-515-5p	1.16960	0.047827	Up
hsa-miR-513-1-pre	1.20450	0.049643	Up

FC, fold change; miR, microRNA.

Table VI. Differentially expressed microRNAs in the GSE14857 dataset.

Gene	logFC	P-value	Gene regulation
hsa-miR-205	4.02160	0.000121	Down
hsa-miR-591	2.81675	0.000442	Down
hsa-miR-668	2.00971	0.003108	Down
hsa-miR-31	2.31899	0.003232	Down
hsa-miR-578	3.86374	0.011947	Down
hsa-miR-490	1.30685	0.010993	Down
hsa-miR-589	2.49788	0.016980	Down
hsa-miR-499	1.24839	0.032533	Down
hsa-miR-217	3.04896	0.031024	Down
hsa-miR-588	3.08085	0.031731	Down
hsa-miR-570	9.13298	0.018255	Down
hsa-miR-526b <sup>a</sup>	1.74544	0.017158	Up
hsa-miR-767-3p	1.32825	0.017129	Up
hsa-miR-183	1.04655	0.000855	Up
hsa-miR-511	1.54791	0.039622	Up
hsa-miR-600	5.08612	0.024913	Up
hsa-miR-663	1.04562	0.028394	Up
hsa-miR-182 <sup>a</sup>	1.35082	0.033078	Up
hsa-miR-216	2.58817	0.045927	Up
hsa-miR-563	1.01419	0.034812	Up

<sup>a</sup>Denotes the passenger strand of the miRNA. FC, fold change; miR, microRNA.

regulates SQLE expression, with high miR-205 levels found to inhibit SQLE and to suppress cholesterol synthesis. These findings highlighted a strong association between miR-205 expression, AR regulation and PCa progression. Given the

mechanism associated with ceRNAs, we hypothesize that an elevated expression of hsa\_circ\_0006168 may lead to its competitively binding with miR-205, thereby reducing its levels and promoting PCa progression. However, it must be emphasized that this remains merely an inference based on bioinformatics analysis, and the putative direct interaction needs to be rigorously confirmed by future functional experiments, including performing dual-luciferase reporter assays.

In the present study, multivariate Cox regression analysis confirmed TNM stage as an independent predictor of survival. Although high hsa\_circ\_0006168 expression, Gleason score and the presence of bone metastasis were reported to be significant risk factors according to the univariate analysis, they lost prognostic independence when adjusted for TNM stage. This is likely due to collinearity (32), a statistical phenomenon where predictor variables are highly associated. In this context, the TNM staging system is a comprehensive index that already incorporates information on tumor grade and metastatic status, such as Gleason score and bone metastasis. Consequently, its prognostic value is encompassed by the staging system. Far from undermining its biological importance, however, this result suggests that hsa\_circ\_0006168 upregulation may represent a key molecular event in the tumor progression and invasion pathways that determine a higher TNM stage. Future studies are warranted to dissect the precise association between hsa\_circ\_0006168 expression and pathological stage.

Moreover, the present study had several limitations. First, the small, single-center sample size limits the generalizability of the conclusions. Therefore, the findings require validation in a larger, independent cohort to confirm their robustness and rule out overfitting before considering clinical application. Secondly, the proposed molecular mechanism is based solely on bioinformatics. Fully elucidating the biological role of hsa\_circ\_0006168 requires extensive experimental validation, including *in vitro* functional studies in cell lines and *in vivo* animal models, to investigate its impact on tumor progression.

In conclusion, the results of the present study indicate that hsa\_circ\_0006168 is highly expressed in PCa, and that this is associated with tumor malignancy. This suggests that it may be a promising biomarker for the adjuvant diagnosis and prognostic monitoring of PCa.

#### Acknowledgements

Not applicable.

#### Funding

No funding was received.

#### Availability of data and materials

The data generated in the present study may be requested from the corresponding author.

#### Authors' contributions

YD analyzed and interpreted data and wrote the manuscript. MTL designed the study and performed the statistical analysis. NY and LG performed the experiments. LPC conceived

the study and revised the manuscript. All authors have read and approved the final manuscript. LPC and YD confirm the authenticity of all the raw data.

#### Ethics approval and consent to participate

The present study was approved by the Ethics Committee of Nantong First People's Hospital (approval no. 2023-KY007-1). All patients provided written informed consent. The study was performed in accordance with the ethical guidelines of the Declaration of Helsinki.

#### Patient consent for publication

Not applicable.

#### Competing interests

The authors declare that they have no competing interests.

#### References

1. Bray F, Laversanne M, Sung H, Ferlay J, Siegel RL, Soerjomataram I and Jemal A: Global cancer statistics 2022: GLOBOCAN estimates of incidence and mortality worldwide for 36 cancers in 185 countries. *CA Cancer J Clin* 74: 229-263, 2024.
2. US Preventive Services Task Force; Grossman DC, Curry SJ, Owens DK, Bibbins-Domingo K, Caughey AB, Davidson KW, Doubeni CA, Ebell M, Epling JW Jr, *et al*: Screening for prostate cancer: US preventive services task force recommendation statement. *JAMA* 319: 1901-1913, 2018.
3. Qu S, Yang X, Li X, Wang J, Gao Y, Shang R, Sun W, Dou K and Li H: Circular RNA: A new star of noncoding RNAs. *Cancer Lett* 365: 141-148, 2015.
4. Lei M, Zheng G, Ning Q, Zheng J and Dong D: Translation and functional roles of circular RNAs in human cancer. *Mol Cancer* 19: 30, 2020.
5. Li S, Hu W, Deng F, Chen S, Zhu P, Wang M, Chen X, Wang Y, Hu X, Zhao B, *et al*: Identification of circular RNA hsa\_circ\_0001599 as a novel biomarker for large-artery atherosclerotic stroke. *DNA Cell Boil* 40: 457-468, 2021.
6. Lv J, Ren L, Han S, Zhang J, Zhao X, Zhang Y, Fang H, Zhang L, Yang H, Wang S, *et al*: Peripheral blood hsa-circRNA5333-4: A novel biomarker for myasthenia gravis. *Clin Immunol* 224: 108676, 2021.
7. Shi J, Liu C, Chen C, Guo K, Tang Z, Luo Y, Chen L, Su Y and Xu K: Circular RNA circMBOAT2 promotes prostate cancer progression via a miR-1271-5p/mTOR axis. *Aging (Albany NY)* 12: 13255-13280, 2020.
8. Shi Y, Guo Z, Fang N, Jiang W, Fan Y, He Y, He Y, Ma Z and Chen Y: hsa\_circ\_0006168 sponges miR-100 and regulates mTOR to promote the proliferation, migration and invasion of esophageal squamous cell carcinoma. *Biomed Pharmacother* 117: 109151, 2019.
9. Wang T, Mao P, Feng Y, Cui B, Zhang B, Chen C, Xu M and Gao K: Blocking hsa\_circ\_0006168 suppresses cell proliferation and motility of human glioblastoma cells by regulating hsa\_circ\_0006168/miR-628-5p/IGF1R ceRNA axis. *Cell Cycle* 20: 1181-1194, 2021.
10. Livak KJ and Schmittgen TD: Analysis of relative gene expression data using real-time quantitative PCR and the 2(-Delta Delta C(T)) method. *Methods* 25: 402-408, 2001.
11. Chen D, Lu X, Yang F and Xing N: Circular RNA circHIPK3 promotes cell proliferation and invasion of prostate cancer by sponging miR-193a-3p and regulating MCL1 expression. *Cancer Manag Res* 11: 1415-1423, 2019.
12. Gleason DF: Classification of prostatic carcinomas. *Cancer Chemother Rep* 50: 125-128, 1966.
13. Verma S, Pandey M, Shukla GC, Singh V and Gupta S: Integrated analysis of miRNA landscape and cellular networking pathways in stage-specific prostate cancer. *PLoS One* 14: e0224071, 2019.

14. Schaefer A, Jung M, Mollenkopf HJ, Wagner I, Stephan C, Jentzmik F, Miller K, Lein M, Kristiansen G and Jung K: Diagnostic and prognostic implications of microRNA profiling in prostate carcinoma. *Int J Cancer* 126: 1166-1176, 2010.
15. Amin MB, Edge SB, Greene FL, Byrd DR, Brookland RK, Washington MK, Gershenwald JE, Compton CC, Hess KR, Sullivan DC, *et al* (eds): *AJCC Cancer Staging Manual*. 8th edition. Springer, New York, NY, 2017.
16. Sobel RE and Sadar MD: Cell lines used in prostate cancer research: A compendium of old and new lines-part 1. *J Urol* 173: 342-359, 2005.
17. Le TK, Duong QH, Baylot V, Fargette C, Baboudjian M, Colleaux L, Taieb D and Rocchi P: Castration-resistant prostate cancer: From uncovered resistance mechanisms to current treatments. *Cancers (Basel)* 15: 5047, 2023.
18. Watson PA, Arora VK and Sawyers CL: Emerging mechanisms of resistance to androgen receptor inhibitors in prostate cancer. *Nat Rev Cancer* 15: 701-711, 2015.
19. Yang Z, Qu CB, Zhang Y, Zhang WF, Wang DD, Gao CC, Ma L, Chen JS, Liu KL, Zheng B, *et al*: Dysregulation of p53-RBM25-mediated circAMOTL1L biogenesis contributes to prostate cancer progression through the circAMOTL1L-miR-193a-5p-Pcdha pathway. *Oncogene* 38: 2516-2532, 2019.
20. Ofner H, Kramer G, Shariat SF and Hassler MR: TP53 deficiency in the natural history of prostate cancer. *Cancers (Basel)* 17: 645, 2025.
21. Teroerde M, Nientiedt C, Duensing A, Hohenfellner M, Stenzinger A and Duensing S: Chapter 8: Revisiting the role of p53 in prostate cancer. In: *Prostate Cancer*. Bott SRJ and Ng KL (eds). Exon Publications, Brisbane, Australia, pp 113-123, 2021.
22. To KKW, Zhang H and Cho WC: Competing endogenous RNAs (ceRNAs) and drug resistance to cancer therapy. *Cancer Drug Resist* 7: 37, 2024.
23. Memczak S, Jens M, Elefsinioti A, Torti F, Krueger J, Rybak A, Maier L, Mackowiak SD, Gregersen LH, Munschauer M, *et al*: Circular RNAs are a large class of animal RNAs with regulatory potency. *Nature* 495: 333-338, 2013.
24. Bartel DP: MicroRNAs: Genomics, biogenesis, mechanism, and function. *Cell* 116: 281-297, 2004.
25. Hansen TB, Jensen TI, Clausen BH, Bramsen JB, Finsen B, Damgaard CK and Kjems J: Natural RNA circles function as efficient microRNA sponges. *Nature* 495: 384-388, 2013.
26. Xu S, Lian Z, Zhang S, Xu Y and Zhang H: CircGNG4 promotes the progression of prostate cancer by sponging miR-223 to enhance EYA3/c-myc expression. *Front Cell Dev Biol* 9: 684125, 2021.
27. Chao F, Song Z, Wang S, Ma Z, Zhuo Z, Meng T, Xu G and Chen G: Novel circular RNA circSOBP governs amoeboid migration through the regulation of the miR-141-3p/MYPT1/p-MLC2 axis in prostate cancer. *Clin Transl Med* 11: e360, 2021.
28. Feng Y, Yang Y, Zhao X, Fan Y, Zhou L, Rong J and Yu Y: Circular RNA circ0005276 promotes the proliferation and migration of prostate cancer cells by interacting with FUS to transcriptionally activate XIAP. *Cell Death Dis* 10: 792, 2019.
29. Gandellini P, Folini M, Longoni N, Pennati M, Binda M, Colecchia M, Salvioni R, Supino R, Moretti R, Limonta P, *et al*: miR-205 exerts tumor-suppressive functions in human prostate through down-regulation of protein kinase cepsilon. *Cancer Res* 69: 2287-2295, 2009.
30. Hagman Z, Hafliadottir BS, Ceder JA, Larne O, Bjartell A, Lilja H, Edsjö A and Ceder Y: miR-205 negatively regulates the androgen receptor and is associated with adverse outcome of prostate cancer patients. *Br J Cancer* 108: 1668-1676, 2013.
31. Kalogirou C, Linxweiler J, Schmucker P, Snaebjornsson MT, Schmitz W, Wach S, Krebs M, Hartmann E, Pühr M, Müller A, *et al*: MiR-205-driven downregulation of cholesterol biosynthesis through SQLE-inhibition identifies therapeutic vulnerability in aggressive prostate cancer. *Nat Commun* 12: 5066, 2021.
32. Gregorich M, Strohmaier S, Dunkler D and Heinze G: Regression with highly correlated predictors: Variable omission is not the solution. *Int J Environ Res Public Health* 18: 4259, 2021.



Copyright © 2026 Ding *et al*. This work is licensed under a Creative Commons Attribution-NonCommercial-NoDerivatives 4.0 International (CC BY-NC-ND 4.0) License.